Viscoelastic Hydrogel Microfibres Exploiting Cucurbit[8]uril Host-guest Chemistry and Microfluidics

Zhi-Jun Meng,[†,‡] *Ji Liu,*[*,§,⊥] *Ziyi Yu,*[‡] *Hantao Zhou,*[#] *Xu Deng,*[*,†] *Chris Abell* [*,‡] *and Oren A. Scherman* [*,§]

[†] Institute of Fundamental and Frontier Sciences, University of Electronic Science and Technology of China, Chengdu, 610054, China.

[‡] Department of Chemistry, University of Cambridge, Lensfield Road, Cambridge, CB2 1EW, UK.

[⊥] Department of Mechanical and Energy Engineering, Southern University of Science and Technology, Shenzhen 518055, P. R. China.

[#] College of Chemistry and Molecular Engineering, Peking University, Beijing 100871, P. R. China.

[§] Melville Laboratory for Polymer Synthesis, Department of Chemistry, University of Cambridge, Lensfield Road, Cambridge, CB2 1EW, UK.

ABSTRACT: Fibre-shaped soft constructs are indispensable building blocks for various 3D functional objects such as hierarchical structures within the human body. The design and fabrication of such hierarchically-structured soft materials, however, are often challenged by the trade-off between stiffness, toughness and continuous production. Here, we describe a microfluidic platform to continuously fabricate double network hydrogel microfibres with tuneable structural, chemical and mechanical features. Construction of the double network microfibres is accomplished through the incorporation of dynamic cucurbit[*n*]uril host-guest interactions, as energy dissipation

moieties, within an agar-based brittle network. These microfibres exhibit an increase in fracture stress, stretchability and toughness by two to three orders of magnitude compared to the pristine agar network, while simultaneously gaining recoverable hysteretic energy dissipation without sacrificing mechanical strength. This strategy of integrating a wide range of dynamic interactions with the breadth of natural resources could been used in the preparation of functional hydrogels, providing a versatile approach towards the continuous fabrication of soft materials with programmable functions.

KEYWORDS: Microfluidic, Hydrogel microfibres, Supramolecular network, Curcutbit[*n*]uril, Self-healing.

INTRODUCTION

Hydrogels are essentially versatile building blocks in living materials, with live creatures as representative prototypes of hydrogel-embodied adaptive machines.[1–6] The intricacy and vast diversity found in biological systems from soft molluscs to hybrid vertebrates, relies on the sophisticated merging of many biological modalities, including gels, tissues, fibres, muscles, tendons and skeletal constructs.[5,7,8] Such biological modalities are exceedingly complex and possess a hierarchically assembled structures featuring a wide length scale, ranging from nano-, micro- to even macroscale, *e.g.* 3D fibre-shaped blood vessels, neural pathways and muscle fibres.[9–12] A high level

of functionality can be achieved in artificial 3D structures through combination of tailor-made molecular engineering and structural complexity formulation.[8] Although technologically incomparable to the high-level complexity of a natural system, these artificial counterparts have sparked the new generation of hierarchically structured functional materials exploited in advanced actuators, soft machines, flexible electronics, and artificial cellular constructs for tissue engineering, *etc*.[3, 4, 13–22]

Inspired by the 3D elongated structure of neural pathways and blood vessels, meter-long hydrogel microfibres have been successfully prepared through continuous microfluidic fabrication relying on the diffusion of Ca^{2+} into an alginate flow, as well as ionic crosslinking of alginate backbones.[10, 11, 23–25] Unfortunately, alginate/Ca^{2+} systems exhibit low mechanical strength (fracture energies < 10 J m^{-2}),[2] which has posed challenges for their applications. Recently, significant progress has been made toward hydrogel networks with outstanding toughness, resilience, elasticity, as well as stretchability.[5] One example in particular exploits the formulation of double network (DN) constructs, pioneered by Gong and coworkers.[5, 26, 27] DN hydrogels consist of two interpenetrating polymer networks with contrasting mechanical properties, where the first network is highly stretched and densely cross-linked (stiff and brittle), and the second is flexible and sparsely cross-linked (soft and stretchable).[5, 26]

Herein, we report the design rationale for tough and highly-stretchable hydrogel microfibres through microfluidics as outlined in **Figure 1a** (see Supplementary Experimental Part for the detailed fabrication process). The initial step involved the formation of hydrogel microfibres from a hot aqueous solution, consisting of agar and

acrylamide-based monomer precursors. Prompt and effective cooling of the hot solution (inner tubular capillary, 700 mm) with ice water (external square capillary, 1000 mm) induced the rapid gelation of agar phase, leading to the formation of first network (**ESI Figure S1**). Here, the sharp thermal transition induces agar network formation, enabling continuous fabrication of meter-long and transparent microfibres (**Figure 1b**), similar to the alginate/Ca^{2+} system based on multiple laminar flow.[10] However, different from the *in situ* solidification of alginate flow relying on diffusion/penetration of Ca^{2+},[10, 11, 23–25] which resulted in an inhomogeneous gradient, thermo-induced gelation of agar can be readily manipulated without any segregated microstructures. A subsequent UV-induced radical polymerization (365 nm, 8 W, 1 h, 0 °C) of acrylamide (AAm)-based monomer precursors is then carried out to generate the second hydrogel network (**Figure 1c**). The monomer precursors used here consist of a 95:5 mixture of hydrophilic acrylamide and 1-benzyl-3-vinylimidazolium bromide (BVIm), which serves as a supramolecular crosslinker upon complexation with cucurbit[8]uril (CB[8]) in a 2:1 manner ($K_{a1} = 4.21\times10^7$ M^{-1}, $K_{a2} = 4.25\times10^5$ M^{-1}),[15, 22] yielding a CB[8] supramolecular hydrogel network (**Figure 1a**). Homogeneous and transparent DN hydrogel microfibres are thus obtained (**Figure 1d**), other than core-sheath structure as reported by Liu and coworkers.[6] Moreover, our strategy here does not involve those multi-step manipulations such as the monomer soaking and afterword polymerization.[26] Our straightforward strategy represents a modular synthetic approach to a diverse range of DN microfibres with tuneable polymer properties, by manipulating the monomer composition,[28] which is

not the theme of our current work.

As revealed in our previous works, [29, 30] incorporation of dynamic CB[8] host-guest complexes imparts the hydrogel networks with remarkable toughness and energy dissipation through reversible dissociation, while subsequent reformation of the ternary complexes lead to immediate recovery of mechanical properties and prompt self-healing at room temperature. In contrast, the agar network is constructed through the association and re-organization of coil-*to*-helix transitions, leading to a stiff and brittle network through helical bundles. Coupling these two disparate networks into one entity could generate a tough DN hydrogel. Tensile tests were conducted to probe the mechanical performance of DN microfibers, while hydrogel microfibres without CB[*n*] or alternatively with the smaller CB[7] macrocycle as well as pristine agar were used as controls. DN hydrogel microfibres exhibited excellent stretchability over 18× their original length (**Figure 2a**, **Figure 2d** and **ESI Supplementary Movie S1**). In a sharp contrast, all controls were too brittle to stretch (**Figure 2a** and **ESI Supplementary Movie S2**), with a fracture strain below 40%. The extreme stretchability and outstanding toughness of the DN hydrogel microfibres could be directly attributed to force-induced dissociation of the CB[8] ternary complexes dissipating local stress, as well as spontaneous re-formation of the complexes, maintaining the tensile stress and strain. [15, 22]

It is important to note that all the microfibres (including the three controls) exhibited comparable Young's moduli (slope measured within 5% strain), which confirms that the material stiffness was dominated by the agar network (**Figure 2b**).

However, the fracture stress of the Agar/CB[8] DN hydrogel microfibres was > 4× that of the CB[7] control, > 6× the control without any CB[*n*], and > 20× that of pristine agar fibers (**Figure 2a** and **Figure 2c**). The toughness of the agar/CB[8] DN hydrogel microfibre is estimated as 4.02 MJ m^{-3}, which is > 470× that of the CB[7] control (8.49×10^{-3} MJ m^{-3}), and > 530× the control without CB[*n*] (7.5×10^{-3} MJ m^{-3}), and > 2800× that of pristine agar microfibre (1.43×10^{-3} MJ m^{-3}), corroborating a substantial increase in the toughness of the DN microfibres (**Figure S3**). On the other hand, the fracture strain (elongation at break) increased by over two orders of magnitude. In light of its extreme stretchability, the cross-sectional area of the DN microfibre changed substantially during stretching, therefore, a further plot of true stress ($\sigma_{true} = \sigma_{nominal} \times (1+\lambda)$) versus strain is more informative, assuming that the hydrogel is not compressible. As shown in **Figure 2b**, σ_{true} at fracture reached as high as 8 MPa, > 20× $\sigma_{nominal}$, and two orders of magnitude greater than σ_{true} of the control fibers (**Figure 2b** and **ESI Figure S2**). Here we did not compare the mechanical properties between our hydrogel microfibers and the bulk hydrogel, due to their different polymerization conditions. Most reported double network hydrogels, for example agar/PAAm DN hydrogel by Zheng and coworkers,[31] were polymerized under inert conditions after rigorous removal of oxygen, thus yielding a much more regular network. In our case, fiber production was conducted in air, and any interference of oxygen during polymerization was readily overcome by increasing the amount of initiator. This readily led to hydrogel microfibers with satisfactory mechanical performance and high efficiency with lower energy consumption.

While a few reports have exploited the generation of hydrogel microfibres using microfluidics,[24] most of them focused on the generation of alginate/Ca^{2+} microfibres;[10, 11, 23, 25] our work here is the first report dedicated to tough and stretchable hydrogel microfibres through host-guest molecular engineering. Such methodology serves as a versatile toolbox, which can be readily extended to a wide variety of hydrogel microfibres with designed and programmable physical, chemical and mechanical performance.

To ascertain the nonlinear and viscoelastic behavior of the DN hydrogel microfibres at large deformation, uniaxial stretching experiments were performed at various stretching rates (**Figure 3a**). The mechanical properties depend strongly with stretching rate, which are typical for supramolecular hydrogel networks.[2, 5, 15, 22] A clear yielding phenomenon can be observed at a strain of *ca*. 70% with the yield stress increasing from 0.13 MPa (100 mm min^{-1}) to 0.25 MPa (600 mm min^{-1}). When the stretching rate increased, a slight decrease in the fracture strain was detected, however, accompanying with an increase in fracture stress and Young's modulus (**Figure 3b**). This viscoelasticity profile is similar to that observed for the pure CB[8] supramolecular hydrogel network (without any agar),[15, 22] arising from time-dependent dynamic dissociation and re-association of CB[8] host-guest complexes in the network.

Another distinctive and advantageous feature arising from supramolecular interactions in the network is their capability to undergo spontaneous dissociation/association imparting both microstructural self-recovery and

(macroscopic) bulk material self-healing. Stress-strain profiles under consecutive cyclic tensile tests (10-1500% strain, **Figure 3c** and **ESI Figure S4-S10**) demonstrated appreciable hysteresis between each loading cycle. Notable increases in hysteresis energy (the energy consumed due to internal bond failure) reflect the amount of energy dissipation through force-induced dissociation of the ternary complexes. A substantial decrease in modulus was observed (**Figure 3d**, green trace to black trace) upon immediate stretching of a DN microfibre sample following a cyclic tensile test (strain 250%, **Figure 3d**, purple trace), however, the material displayed self-repairing after 60 min at room temperature (**Figure 3d**, orange trace). Zheng and co-workers[31] claimed that, in the agar/PAAm double network, the agar first-network ruptured into small clusters and dissipated energy, while the PAAm second-network remained intact. Here, in the case of the agar/CB[8] DN, while it is impossible to differentiate the specific role of each network directly during the mechanical tests, we speculate that both networks, the agar and CB[8] single network, synergistically contribute to the overall energy dissipation behavior, through both rupturing of the agar network into small clusters and the reversible association/dissociation of the CB[8] host-guest complexes, respectively.

While microscopic self-repair of the DN hydrogel microfibres is clearly evident (**Figure 3c-d**), further investigation into macroscopic self-healing was carried out through two different tests. A sample was cut with a blade (in approximately half of its original dimension, dimension, **Figure 4a, b** and **ESI Figure S11**) and brought back into contact with itself to demonstrate direct self-healing (**Figure 4d-i**), while another test took two different samples and 'welded' them together through contact, displaying

indirect self-healing or adhesion (**Figure 4d-ii**). Previous reports have revealed that the self-healing performance of agar/polyacrylamide-based DN hydrogels could be only achieved favorably through exposure to elevated temperature, *e.g.* 95 °C, in order to activate melting, re-arrangement and re-formation of the agar network.[31,32] Moreover, unfavorable self-healing at room temperature was reported by Gong and co-workers,[33] since the presence of covalent cross-links dramatically inhibited polymer chain mobility.[34] Surprisingly, in the case of agar/CB[8] DN hydrogel microfibres, substantial self-healing at room temperature was observed for both self-healed and adhered samples, sustaining stretching over 13× their original dimensions. As described in **Figure 4c**, self-healing and interfacial adhesion is promoted by the second CB[8] network within which the re-complexation or re-arrangement of the ternary complexes serve to dramatically accelerate re-construction of the network,[22] thus recovering the macroscopic mechanical properties. While complete self-healing/recovery was observed in the pure CB[8] hydrogel network,[21] partial self-healing could be quantified with a healing efficiency (defined as the ratio of tensile work for the healed samples to that of the original samples) up to 70% in direct self-healing and 40% in adhesion, respectively. The difference in self-healing efficiency between the direct self-healing and adhesion here might be interpreted by the polymer chain state. Normally, the hydrogel surface possesses a lower water content than the inner part, due to the surface water loss, especially for hydrogel microfibers with a higher surface-volume ratio. Therefore, polymer chains within the hydrogel networks exhibit higher flexibility than those on the surfaces. That is why the new cut surface can self heal faster than the

adhesion between two hydrogel ends. A 'scar' of the cut was still visible under microscopic observation after 12 h (**Figure 4d i-1** and **Figure 4d i-2**), which could be attributed to the limited chain mobility and re-arrangement of the primary agar network. Undoubtedly, an increase in temperature would favor accelerating agar chain mobility, likely leading to a higher degree of self-healing, as demonstrated by Zheng and coworker.[32] In our case, considering the large surface to volume ratio of the microfibre, we did not exploit higher temperature-accelerated self-healing as it would lead to unavoidable water evaporation at elevated temperatures. Nevertheless, the room temperature self-healing of the DN microfibre highlights the beauty of incorporating supramolecular recognition elements, *e.g.* CB[*n*] host-guest chemistry, into the system.

A major challenge in material design is the trade-off between stiffness and extensibility/toughness. Here, we circumvent this inherent trade-off by incorporating sacrificial, reversible CB[*n*] molecular recognition into a brittle agar hydrogel microfibre. Compared with pristine agar microfibres or previously-reported alginate/Ca^{2+} microfibres, the DN microfibres produced here exhibit two orders of magnitude increase in fracture stress, stretchability, and toughness, while gaining recoverable hysteretic energy dissipation. Coexistence of such mechanical characteristics is rare for hydrogel microfibres. Fabrication of these DN hydrogel microfibres represents a powerful and facile method to produce anisotropic microscale supramolecular functional materials, holding great promise for myriad applications including artificial silks, tissue engineering, wearable electronic devices and microactuators.

ASSOCIATED CONTENT

Supporting Information.

The Supporting Information is available free of charge on the ACS Publications website: Supplementary experimental details; Supplementary Results Figure S1-S11; Supplementary Movie S1 and S2.

AUTHOR INFORMATION

Corresponding Author

Email: liuj9@sustech.edu.cn (J. L.)

E-mail: dengxu@uestc.edu.cn (X. D.)

E-mail: ca26@cam.ac.uk (C. A.)

Email: oas23@cam.ac.uk (O. A. S.)

Notes

The authors declare no competing financial interest.

ACKNOWLEDGMENTS

Z-J. M and X. D. acknowledge the National Natural Science Foundation of China (Grant No. 21603026) and the Max Planck Partner Group grant. J.L. thanks the Marie Curie FP7 SASSYPOL ITN (607602) program and O.A.S thanks the EPRSC (EP/L027151) and Walters–Kundert Trust Next Generation Fellowship for funding.

FIGURES

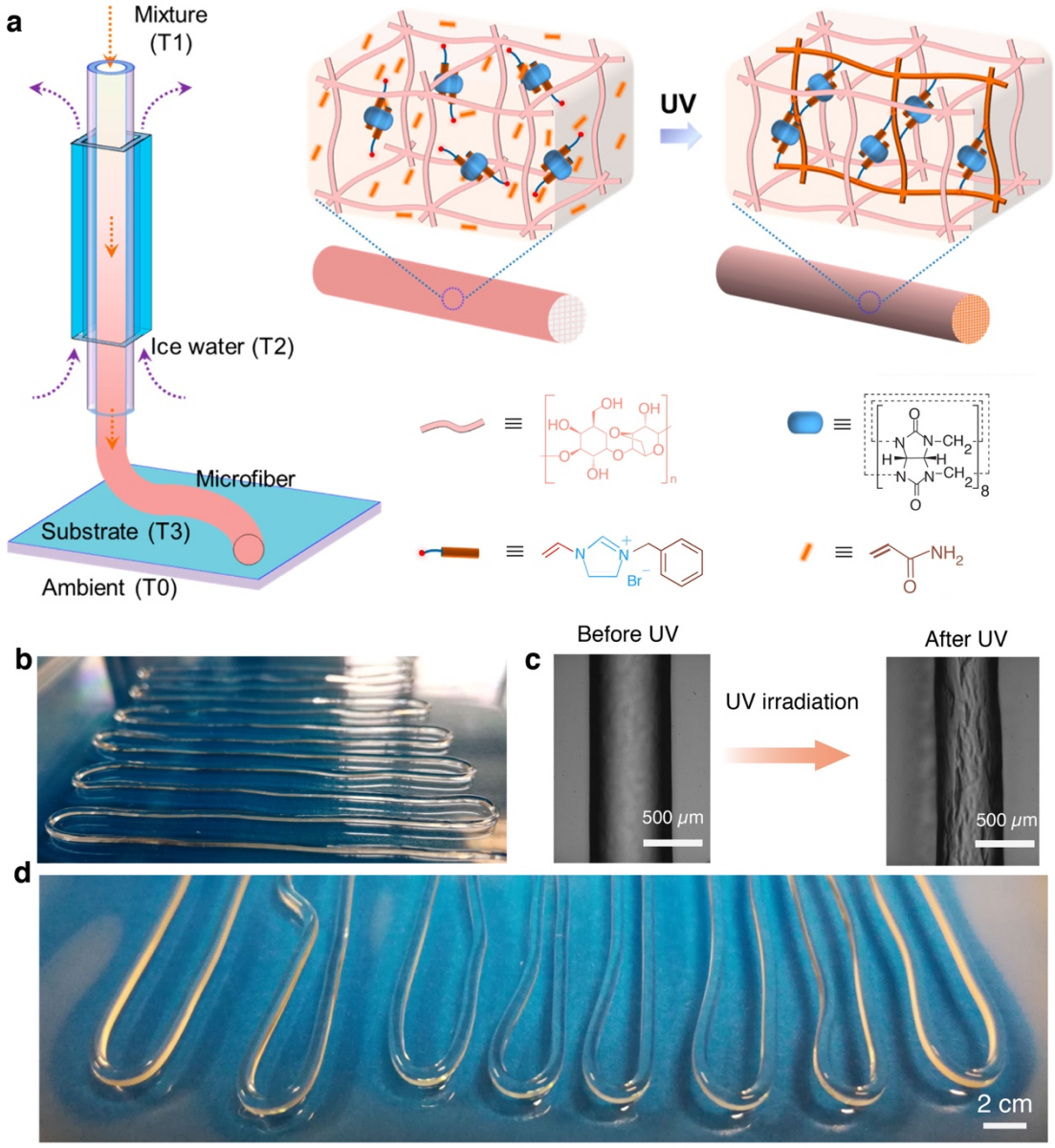

Figure 1. (a) Schematic illustration for continuous fabrication of double network hydrogel microfibres by integrating the microfluidic fabrication and supramolecular host-guest chemistry. A hot mixture solution of agar and an acrylamide-based monomer precursor (T_1 = 50 °C) was injected into the microfluidic channel, while *in situ* cooling with ice water (T_2 = 0 °C) induced the immediate gelation of agar, forming the first hydrogel network (T_0 = 20 °C and T_3 = 0 °C). Further UV-activated radical copolymerization of the acrylamide-based monomer precursor and the BVIm:CB[8]

supramolecular crosslinker led to the second supramolecular hydrogel network. (b) Image of the hydrogel microfibres before UV irradiation. (c) Microscopic images of the hydrogel microfibre before and after UV-activated generation of the second hydrogel network. (d) Image of the hydrogel microfibres after UV irradiation.

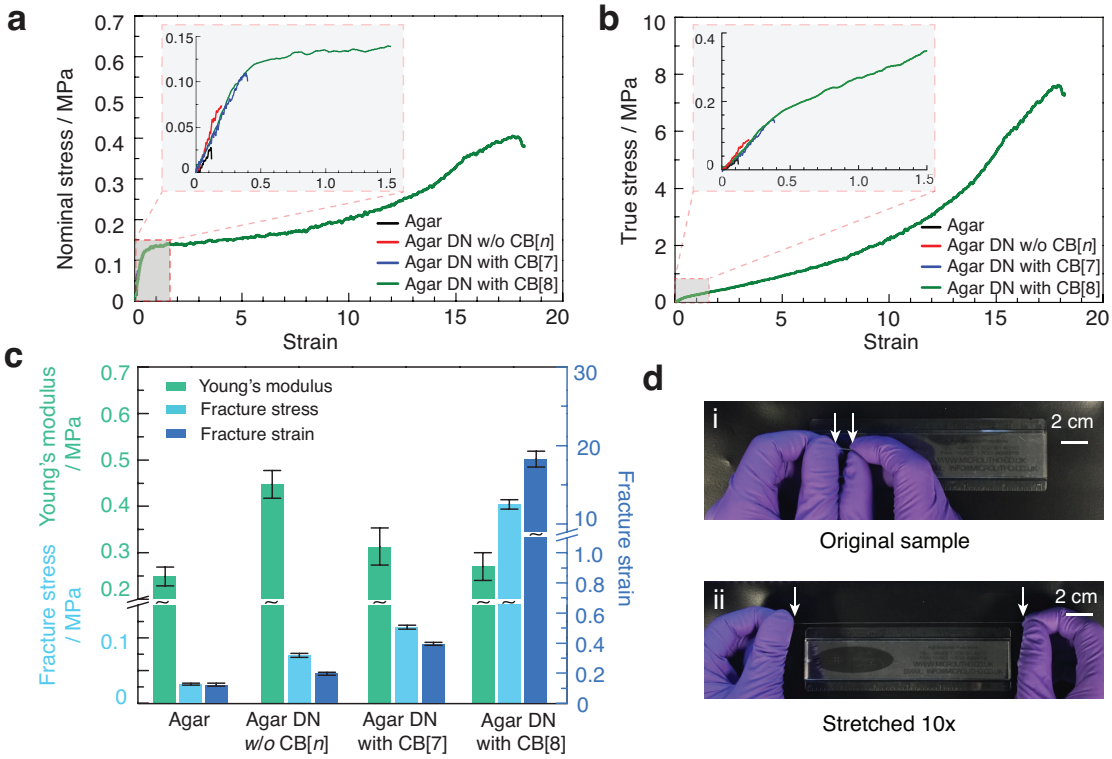

Figure 2. Typical tensile-strain curves of the DN hydrogel microfibres including controls without CB[n], with CB[7], as well as a pure agar fiber, leading to nominal stress (a) and true stress (b) plots (deformation rate: 100 mm min^{-1}). True strain is defined as $\sigma_{true} = \sigma_{nominal} \times (1+\lambda)$. (c) Summary of Young's moduli, fracture stress and fracture strain for each hydrogel microfibre sample. (d) Manual stretching of an agar/CB[8] DN hydrogel microfibre sample (i) by 10× (ii).

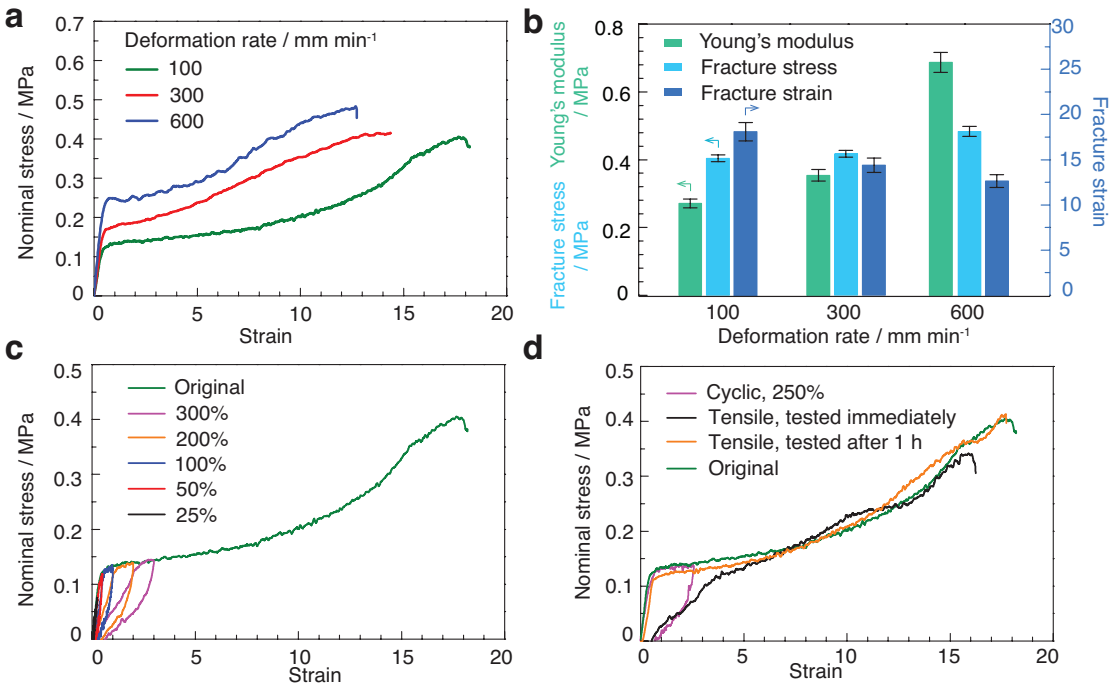

Figure 3. (a) Deformation-rate-dependent tensile stress-strain curves of the agar/CB[8] DN hydrogel microfibres and (b) reliance of mechanical parameters (Young's moduli, fracture stress and fracture strain) on deformation rate. (c) Consecutive tensile loading-unloading cycles of an agar/CB[8] DN microfibre sample, following gradually-increased cyclic strains (25-300%). Marginal overlapping of the cyclic curves with the original tensile curve corroborates high-level reproducibility. (d) Stress-strain plots of cyclic tensile tests at a strain of 250%, followed by an immediate second tensile test, or after a waiting time of 1 h, with the original tensile test curve for comparison.

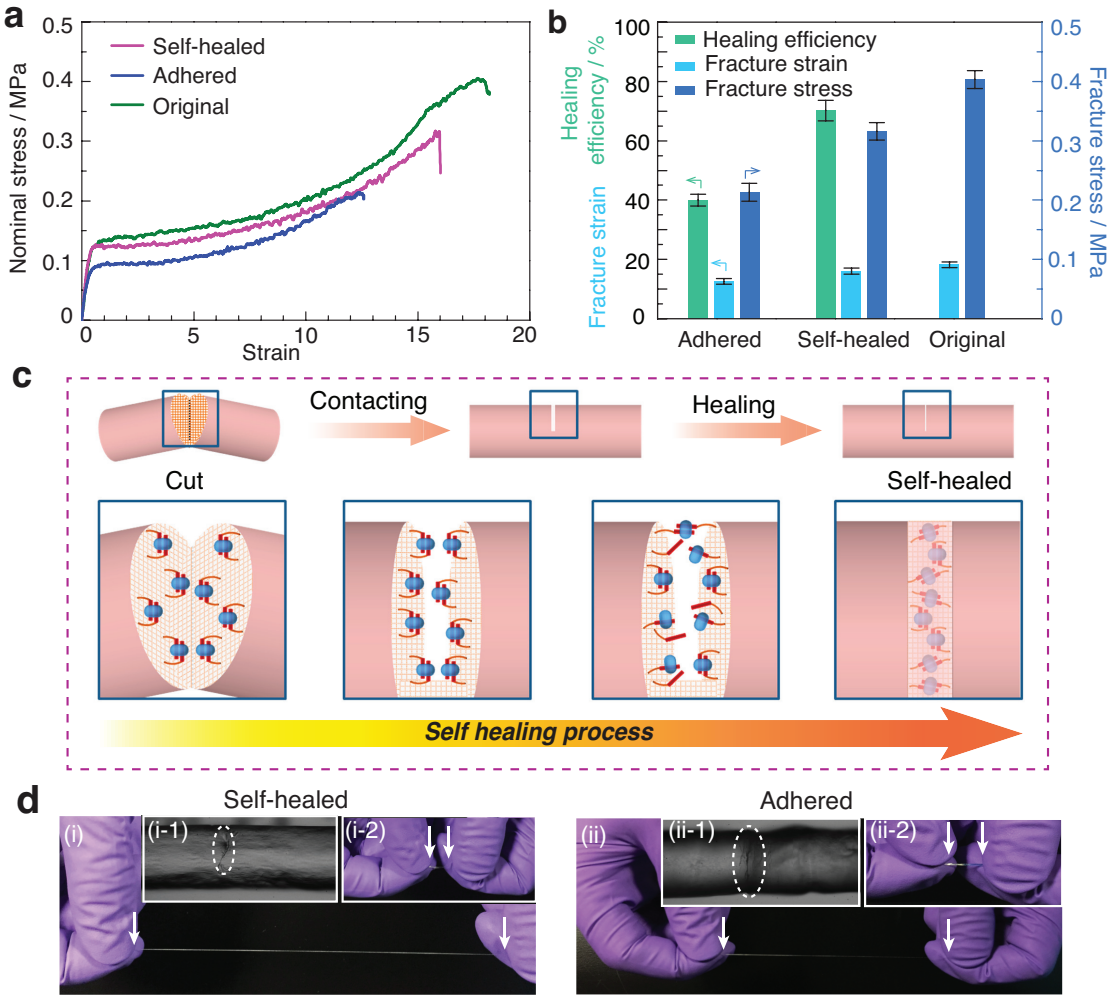

Figure 4. (a) Stress-strain curve of self-healed and adhered DN hydrogel microfibre samples. The self-healed sample was obtained by cutting a sample (approximately half of the original dimension) and brought into direct contact for 12 h at room temperature; while an adhered sample was made from two different microfibre samples. (b) Comparison of fracture strain, fracture stress and healing efficiency for the self-healed and adhered samples. (c) Schematic illustration of macroscopic self-healing promoted by the second CB[8] network, within which the re-association or re-arrangement of the ternary complexes dramatically accelerate the re-construction of the dynamic CB[8] hydrogel network. (d) Manual stretching of a self-healed (i) and adhered (ii) hydrogel microfibre sample. Inset: microscopic images showing the location of the cut, which is still visible after 12 h. For the adhered test, one of the samples was stained with a small amount of calcium blue to differentiate it from the self-healed sample.

REFERENCES

1. Maier, G. P.; Rapp, M. V.; Waite, J. H.; Israelachvili, J. N.; Butler, A. Adaptive Synergy between Catechol and Lysine Promotes Wet Adhesion by Surface Salt Displacement. *Science* **2015**, 349, 628–632, DOI: 10.1126/science.aab0556.

2. Sun, J. Y.; Zhao, X. H.; Illeperuma, W. R. K.; Chaudhuri, O.; Oh, K. H.; Mooney, D. J.; Vlassak, J. J.; Suo, Z. G. Highly Stretchable and Tough Hydrogels. *Nature* **2012**, 489, 133–136, DOI: 10.1038/nature11409.

3. Li, J.; Celiz, A. D.; Yang, J.; Yang, Q.; Wamala, I.; Whyte, W.; Seo, B. R.; Vasilyev, N. V.; Vlassak, J. J.; Suo, Z.; Mooney, D. J. Tough Adhesives for Diverse Wet Surfaces. *Science* **2017**, 357, 378–381, DOI: 10.1126/science.aah6362.

4. Liu, X.; Liu, J.; Lin, S.; Zhao, X. Hydrogel Machines. *Mater. Today*. 2020, in press, DOI: 10.1016/j.mattod.2019.12.026.

5. Gong, J. P. Materials Both Tough and Soft. *Science* **2014**, 344, 161–162, DOI: 10.1126/science.1252389.

6. Dou, Y. Y; Wang, Z. P.; He, W. Q.; Jia, T. J.; Liu, Z. J.; Sun, P. C.; Wen, K.; Gao E. L.; Zhou, X. Z.; Hu, X. Y.; Li, J. J.; Fang S. L.; Qian, D.; Liu, Z. F. Artificial Spider Silk from Ion-Doped and Twisted Core-Sheath Hydrogel Fibres. *Nat. Commun.* **2019**,10, 5293, DOI:10.1038/s41467-019-13257-4.

7. Green, J. J.; Elisseeff, J. H. Mimicking Biological Functionality with Polymers for Biomedical Applications. *Nature* **2016**, 540, 386–394, DOI: 10.1038/nature21005.

8. Lutz, J. F.; Lehn, J. M.; Meijer, E. W.; Matyjaszewski, K. From Precision Polymers to Complex Materials and Systems. *Nat. Rev. Mater.* **2016**, 1, 16024, DOI: 10.1038/natrevmats.2016.24.

9. Frederix, P. W. J. M.; Scott, G. G.; Abul-Haija, Y. M.; Kalafatovic, D.; Pappas, C. G.; Javid, N.; Hunt, N. T.; Ulijn, R. V.; Tuttle, T. Exploring the Sequence Space for (Tri-)peptide Self-assembly to Design and Discover. *Nat. Chem.* **2015**,7, 30-37, DOI: 10.1038/nchem.2122.

10. Onoe, H.; Okitsu, T.; Itou, A.; Kato-Negishi, M.; Gojo, R.; Kiriya, D.; Sato, K.; Miura, S.; Iwanaga, S.; Kuribayashi-Shigetomi, K.; Matsunaga, Y. T.; Shimoyama, Y.; Takeuchi, S. Metre-long Cell-Laden Microfibres Exhibit Tissue Morphologies and Functions. *Nat. Mater.* **2013**, 12, 584–590, DOI: 10.1038/nmat3606.

11. Kang, E.; Jeong, G. S.; Choi, Y. Y.; Lee, K. H.; Khademhosseini, A.; Lee, S. H. Digitally Tunable Physicochemical Coding of Material Composition and Topography in Continuous Microfibres. *Nat. Mater.* **2011**, 10, 877–883, DOI: 10.1038/nmat3108.

12. Leong, M. F.; Toh, J. K. C.; Du, C.; Narayanan, K.; Lu, H. F.; Lim, T. C.; Wan, A. C. A.; Ying, J. Y. Patterned Prevascularised Tissue Constructs by Assembly of Polyelectrolyte Hydrogel Fibres. *Nat. Commun.* **2013**, 4, 2353, DOI: 10.1038/ncomms3353.

13. Annabi, N.; Zhang, Y. N.; Assmann, A.; Sani, E. S.; Cheng, G.; Lassaletta, A. D.; Vegh, A.; Dehghani, B.; Ruiz-Esparza, G. U.; Wang, X. C.; Gangadharan, S.; Weiss, A. S.; Khademhosseini, A. Engineering a Highly Elastic Human Protein-Based Sealant for Surgical Applications. *Sci. Transl. Med.* **2017**, 9, eaai7466, DOI: 10.1038/ncomms3353.

14. Wu, Y. C.; Shah, D. U.; Liu, C. Y.; Yu, Z. Y.; Liu, J.; Ren, X. H.; Rowland, M. J.; Abell, C.; Ramage, M. H.; Scherman, O. A. Bioinspired Supramolecular Fibers Drawn from a Multiphase Self-Assembled Hydrogel. *Proc. Natl. Acad. Sci. U.S.A.* **2017**, 114, 8163–8168, DOI: 10.1073/pnas.1705380114.

15. Liu, J.; Tan, C. S. Y.; Yu, Z. Y.; Li, N.; Abell, C.; Scherman, O. A. Tough Supramolecular Polymer Networks with Extreme Stretchability and Fast Room-Temperature Self-Healing. *Adv.Mater.* **2017**, 29, 1605325, DOI: 10.1002/adma.201605325.

16. Guo, J.; Liu, X.; Jiang, N.; Yetisen, A. K.; Yuk, H.; Yang, C.; Khademhosseini, A.; Zhao, X.; Yun, S. H. Highly Stretchable, Strain Sensing Hydrogel Optical Fibers. *Adv. Mater.* **2016**, 28, 10244–10249, DOI: 10.1002/adma.201603160.

17. Zhang, Y. S.; Khademhosseini, A. Advances in Engineering Hydrogel*s*. *Science* **2017**, 356, eaaf3627, DOI: 10.1126/science.aaf3627.

18. Liu, J.; Scherman, O. A. Cucurbit[n]uril Supramolecular Hydrogel Networks as Tough and Healable Adhesives. *Adv. Funct. Mater.* **2018**, 28, 1800848, DOI: 10.1002/adfm.201800848.

19. Liu, X.; Steiger, C.; Lin, S.; Parada, G.A.; Liu, J.; Chan, H.F.; Yuk, H.; Phan, N.V.; Collins, J.; Tamang, S; Traverso, G.; Zhao, X; 2019. Ingestible Hydrogel Device. *Nat. Commun.* **2019**, 10, 493, DOI: 10.1038/s41467-019-08355-2.

20. Liu, J.; Tan, C. S. Y.; Scherman, O. A. Dynamic Interfacial Adhesion through Cucurbit[n]uril Molecular Recognition. *Angew. Chem. Int. Ed.* **2018**, 130, 8992-8996, DOI: 10.1002/ange.201800775.

21. Lin, S.; Liu, J.; Liu, X.; Zhao, X. Muscle-Like Fatigue-Resistant Hydrogels by Mechanical Training. *Proc. Natl. Acad. Sci. USA*, **2019**, 116, 10244-10249, DOI: 10.1073/pnas.1903019116.

22. Liu, J.; Tan, C. S.; Yu, Z.; Lan, Y.; Abell, C.; Scherman, O. A. Biomimetic Supramolecular Polymer Networks Exhibiting both Toughness and Self-Recovery. *Adv. Mater.* **2017**, 29, 1604951, DOI: 10.1002/adma.201604951.

23. Meng, Z. J.; Wang, W.; Xie, R.; Ju, X. J.; Liu, Z.; Chu, L. Y. Microfluidic Generation of Hollow Ca-Alginate Microfibers. *Lab Chip* **2016**, 16, 2673–2681, DOI: 10.1039/C6LC00640J.

24. Chung, B. G.; Lee, K. H.; Khademhosseini, A.; Lee, S. H. Microfluidic Fabrication of Microengineered Hydrogels and Their Application in Tissue Engineering. *Lab Chip* **2012**, 12, 45–59, DOI: 10.1039/C1LC20859D.

25. Cheng, Y.; Zheng, F.; Lu, J.; Shang, L.; Xie, Z.; Zhao, Y.; Chen, Y.; Gu, Z. Z. Bioinspired Multicompartmental Microfibers from Microfluidics. *Adv. Mater.* **2014**, 26, 5184–5190, DOI: 10.1002/adma.201400798.

26. Gong, J.P.; Katsuyama, Y.; Kurokawa, T.; Osada, Y. Double-Network Hydrogels with Extremely High Mechanical Strength. *Adv. Mater.* **2003**,15, 1155–1158, DOI: 10.1002/adma.200304907.

27. Zhang, H. J.; Sun, T. L.; Zhang, A. K.; Ikura, Y.; Nakajima, T.; Nonoyama, T.; Kurokawa, T.; Ito, O.; Ishitobi, H.; Gong, J. P. Tough Physical Double‐Network Hydrogels Based on Amphiphilic Triblock Copolymers. *Adv. Mater.* **2016**, 28, 4884–4890, DOI: 10.1002/adma.201600466.

28. Liu, J.; Tan, C. S. Y.; Lan, Y.; Scherman, O. A. Toward a Versatile Toolbox for Cucurbit[n]uril-Based Supramolecular Hydrogel Networks Through in situ Polymerization. *J. Polym. Sci. Polym. Chem.* **2017**, 55, 3105–3109, DOI: 10.1002/pola.28667.

29. Liu, J.; Lan, Y.; Yu, Z.; Tan, C.S.Y.; Parker, R.M.; Abell, C.; Scherman, O.A. Cucurbit[*n*]uril-based microcapsules self-assembled within microfluidic droplets: a versatile approach for supramolecular architectures and materials. *Acc. Chem. Res.* **2017**, 50, 208–217, DOI: 10.1021/acs.accounts.6b00429.

30. Tan, C. S. Y.; Liu, J.; Groombridge, A. S.; Barrow, S. J.; Dreiss, C. A.; Scherman, O. A. Controlling Spatiotemporal Mechanics of Supramolecular Hydrogel Networks with Highly Branched Cucurbit[8]uril Polyrotaxanes. *Adv. Funct. Mater.* **2018**, 28, 1702994, DOI: 10.1002/adfm.201702994.

31. Chen, Q.; Zhu, L.; Zhao, C.; Wang, Q.; Zheng, J. A robust, One-Pot Synthesis of Highly Mechanical and Recoverable Double Network Hydrogels Using

Thermoreversible Sol–Gel Polysaccharide. *Adv. Mater.* **2013**, 25, 4171–4176, DOI: 10.1002/adma.201300817.

32. Chen, H.; Liu, Y.; Ren, B.; Zhang, Y.; Ma, J.; Xu, L.; Chen, Q.; Zheng, J. Super Bulk and Interfacial Toughness of Physically Crosslinked Double-Network Hydrogels. *Adv. Funct. Mater.* **2017**, 27, 1703086, DOI: 10.1002/adfm.201703086.

33. Ihsan, A. B.; Sun, T. L.; Kurokawa, T.; Karobi, S. N.; Nakajima, T.; Nonoyama, T.; Roy, C. K.; Luo, F.; Gong, J. P. Self-Healing Behaviors of Tough Polyampholyte Hydrogels. *Macromolecules* **2016**, 49, 4245–4252, DOI: 10.1021/acs.macromol.6b00437.

34. Chen, Q.; Zhu, L.; Chen, H., Yan, H.; Huang, L.; Yang, J.; Zheng, J. A Novel Design Strategy for Fully Physically Linked Double Network Hydrogels with Tough, Fatigue Resistant, and Self‐Healing Properties. *Adv. Funct. Mater.* **2015**, 25, 1598–1607, DOI: 10.1002/adfm.201404357.

GRAPHICAL ABSTRACT

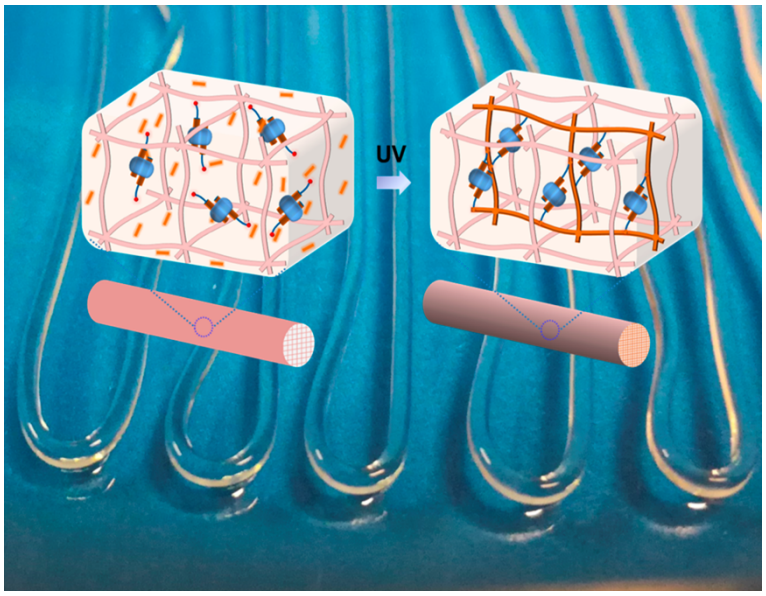

Double network hydrogel microfibres with varying structural, chemical and mechanical features were continuously fabricated through a microfluidic platform. Cooperative incorporation of dynamic cucurbit[8]uril host-guest interactions and agar-based brittle network enables the construction of anisotropic double network microfibres, with exceptional improved fracture stress, extensibility and tensile toughness.